Electronic topological transitions in Zn under compression

Vladimir V. Kechin*
Institute for High Pressure Physics, Troitsk, Moscow oblast, 142190 Russia
(Received 2 August 1999; revised manuscript received 5 September 2000; published 9 January 2001)

The electronic structure of hcp Zn under pressure up to 10 GPa has been calculated self-consistently by means of the scalar relativistic tight-binding linear muffin-tin orbital method. The calculations show that three electronic topological transitions (ETT's) occur in Zn when the c/a axial ratio diminishes under compression. One transition occurs at $c/a \simeq 1.82$ when the ''needles'' appear around the symmetry point K of the Brillouin zone. The other two transitions occur at $c/a \simeq \sqrt{3}$, when the ''butterfly'' and ''cigar'' appear simultaneously both around the L point. It has been shown that these ETT's are responsible for a number of anomalies observed in Zn at compression.

DOI: 10.1103/PhysRevB.63.045119 PACS number(s): 64.70.Kb

I. INTRODUCTION

Zinc and cadmium are unique among the hcp metals, having unusually large c/a axial ratios under ambient conditions (1.856 for Zn and 1.886 for Cd) as compared to the ideal value ($\sqrt{8/3} \simeq 1.633$). Due to this large c/a ratio, many solid-state properties of Zn and Cd are highly anisotropic.

For divalent hcp metals having the c/a ratio close to the ideal one, such as Mg, the Fermi surface contains six elements. Unlike Mg, the Fermi surface of Zn (and Cd) contains only three elements of six (namely, the ''cap,'' ''monster,'' and ''lens''). Consequently, the ''cigar'' and ''butterfly'' near the symmetry point L and the ''needles'' near the symmetry point K of the Brillouin zone are absent.[1]

The axial c/a ratio, the main parameter governing the electronic structure of these metals, decreases under compression toward the ideal ratio due to a high anisotropy of their compressibilities. As the c/a ratio diminishes, new elements of the Fermi surface appear. This electronic topological transition (ETT), or the Lifshitz transition of the $2\frac{1}{2}$ order,[2] can lead to anomalies in transport and thermodynamic properties.[3] In this connection, the study of Zn and Cd under compression is of particular interest.

In 1995, an anomaly in the Mössbauer spectrum of Zn was found at $P \sim 6.6$ GPa and 4.2 K when the Lamb-Mössbauer factor abruptly dropped.[4,5] Based on the full-potential linearized augmented plane-wave calculation, the authors suggested that the giant Kohn anomaly collapse was responsible for the observed phenomenon, due to the ETT at the L point of the Brillouin zone. Shortly thereafter, Takemura[6–8] detected changes in the c/a axial ratio slope at $P \simeq 9.4$ GPa from high precision x-ray powder-diffraction experiments at 300 K up to 126 GPa. Takemura estimated[6] that both of the anomalies, at room and at low temperature, occur at the same axial ratio, $c/a = \sqrt{3}$. These two experimental observations of anomalies have stimulated extensive investigation of Zn both experimentally[9–11] and theoretically.[12–16]

It has long been known that the transport properties of Zn behave unusually under varying pressure or temperature. Thus, the electrical resistance displays an irregular character,[17] and the electrical resistivities curves along the principal axes appear to intersect under pressure.[18] The thermal resistivities exhibit the same ''crossing effects'' at low temperatures.[19] One should also mention the linear thermal-expansion coefficient $\alpha_{\perp}(T)$ sign oscillation at low temperatures.[20] Up to now, there has been no explanation for these experimental data.

We suppose that the electronic structure features of Zn, in the case of the c/a axial ratio change, are responsible for the observed anomalies. In order to elucidate the origin of the anomalies, we performed the calculation of Zn electronic structure under compression.

II. RESULTS AND DISCUSSION

The tight-binding linear muffin-tin orbital method with the atomic-sphere approximation[21–23] was applied to calculating the band structure and the electronic density of state of Zn under pressure up to 16 GPa. The numerical x-ray data of Takemura on the lattice parameters, $a(P)$ and $c(P)$, were used as the input parameters for the calculations.[7,8] The scalar-relativistic description for the valence the states was used. No spin-orbit coupling was taken into account. To obtain reliable results, we applied a dense **k** mesh of 12 000 points in the full Brillouin zone. The main results of the self-consistent calculations are depicted in Figs. 1–4.

The energy-band calculations show that the band levels at the K and L symmetry points of the Brillouin zone of Zn intersect the Fermi energy E_F as the c/a ratio decrease under pressure (Fig. 1). The main contribution to the total density of states at the Fermi energy, $N(E_F)$, comes from p states, which are responsible for an anomalously high c/a axial ratio for Zn. The contributions of s and d states to $N(E_F)$ are almost equal. The details of our electronic structure calculations show a continuous, though slow, transfer of electrons from p to s and d states when c/a decreases. Under pressure, the $3d^{10}$ bandwidth broadens and the gravity center of the d band moves downward with respect to the Fermi energy (Fig. 2).[24–26]

A. ETT at the *K* point of the Brillouin zone

Calculations show that the upper edge E_K of the direct local band gap at the K symmetry point intersects the Fermi

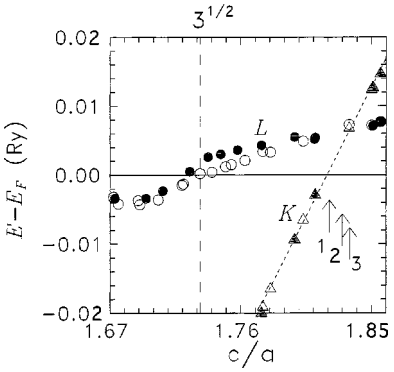

FIG. 1. The energy separations between the Fermi level and the band levels at the symmetry points K (triangles) and L (circles) as a function of c/a. Solid symbols are for hydrostatic conditions (Ref. 8), and the open ones are for slightly nonhydrostatic conditions (Refs. 6 and 7). Arrows indicate the c/a ratios, at which (1) the electrical resistivities $\rho_{\parallel}$ and $\rho_{\perp}$ intersect (Ref. 18); (2) the thermal resistivities $w_{\parallel}$ and $w_{\perp}$ intersect (Ref. 19); (3) the cross-sectional area of the needles is zero (Ref. 27).

level at $c/a \simeq 1.818$ and the ETT (the ''needles'') appear near this point in the third Brillouin zone. Hence, at ambient conditions, the needles are absent in Zn and may exist under pressure or cooling due to a reduction of the c/a axial ratio. (Note that in the nearly-free-electron model the ETT at the K point occurs at $c/a = 1.861$; that is, the needles exist at ambient conditions.)

The cross-sectional area of the needles and its dependence on pressure were measured at 4.2 K by studying the period of the de Haas–van Alfen (dHvA) oscillations.[27,28] The linear extrapolation of the dHvA experiments[27] suggests that the needles appear (disappear) at $c/a \simeq 1.835$ in reasonably good agreement with the present calculations (Fig. 1). Previously, we measured the electrical resistivity of a single Zn crystal at 300 K along the c and a axes, $\rho_{\parallel}$ and $\rho_{\perp}$, respectively, under pressure up to 8 GPa.[18] It was shown that the

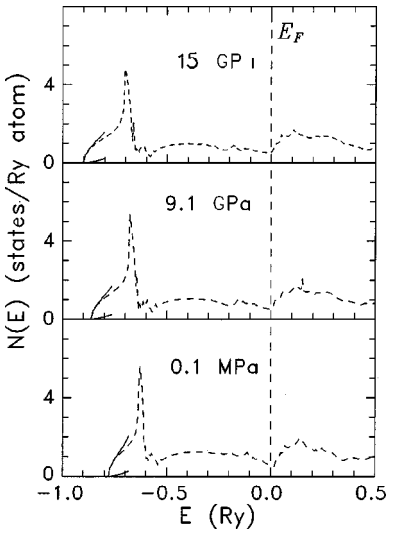

FIG. 2. Density of states of hcp Zn at various pressures. The solid curves are for the total and for the partial p states, the dashed curves are for the partial s states.

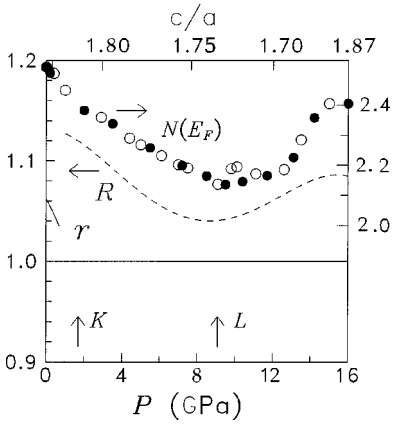

FIG. 3. The calculated total density of states $N(E_F)$ (states/Ry atom) at the Fermi level (circles, see Fig. 1); the dashed curve is for the electrical resistance R (arb. units), data of Lynch and Drickamer (Refs. 17 and 30), and the solid curve is for the ratio of resistivities, $r = \rho_{\parallel}/\rho_{\perp}$ (Ref. 18) of Zn as a function of pressure. Vertical arrows show the pressures, at which electronic topological transitions occur at the K and L symmetry points of the Brillouin zone.

curves for $\rho_{\parallel}$ and $\rho_{\perp}$ intersect at 1.29 GPa ($c/a = 1.821$), and Zn becomes electrically isotropic (Fig. 3). The thermal resistivity for Zn at ambient pressure displays the same ''crossing effect'' at cooling.[19] Namely, the curves of $w_{\parallel}$ and $w_{\perp}$ intersect at $T \approx 30$ K. [It is remarkable that there exists a pronounced peak in the thermopower of Zn for $s_{\parallel}$ and $s_{\perp}$ at the same temperature, $T \approx 30$ K (Ref. 26).] The cooling of Zn up to 30 K is equivalent to its compression up to $\simeq 1.5$ GPa or to the reduction of the axial ratio up to $c/a \simeq 1.828$ (we use the thermal expansion data[20] to estimate the c/a vs temperature dependence). It is obvious that the crossing effects for the electrical and thermal resistivities are of the same origin. Figure 1 shows that both of the effects correlate very well with the ETT at point K. Note that the crossing effect for the thermal resistivity does not occur for Cd.[19] The ETT at the K point for Cd should be expected at higher compression than for Zn and hence cannot be observed at cooling.

Inelastic neutron scattering experiments for Zn at ambient conditions[29] indicate a rapid increase of the group velocity when the phonon wave vector $\mathbf{q} \rightarrow 0$. It is believed that this effect is a result of the giant Kohn anomaly in the long-

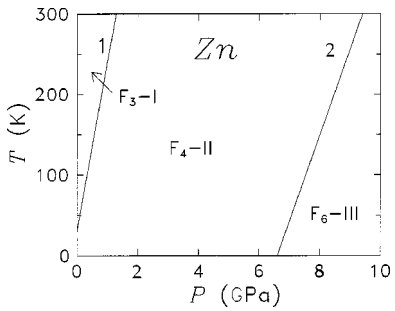

FIG. 4. The T-P diagram of the electronic phases F_k-N in Zn (k is the number of the Fermi-surface elements and N is the ordinal number of phase). Line 1, $c/a = 1.82$ ($E_K = E_F$). Line 2, $c/a = 1.732$ ($E_L = E_F$).

wavelength region and is associated with the energy gap at the L point of the Brillouin zone.[4,5] It should be noted that at $T>30$ K, the Fermi level at the point K also lies inside the local band gap and no electronic state exists at this point (no needles). For this point, the reciprocal-lattice vector $\mathbf{G}_K=(1,1,0)$ satisfies the condition $2k_F=|\mathbf{G}_K|$ for the giant Kohn anomaly existence. The appearance of new sheets of the Fermi surfaces due to the c/a axial ratio reduction destroy the giant Kohn anomaly, thereby modifying the lattice dynamics.

Measurements of the thermal expansion of the single crystals[20] show the oscillatory behavior of the transverse expansion coefficient, $\alpha_\perp(T)$. It becomes negative below 75 K and passes through a minimum at 30 K ($c/a=1.829$), whereas the coefficient parallel to the hexagonal axis, $\alpha_\parallel$, remains large and positive. At $T<8$ K (i.e., over a very narrow range of the $c/a=1.828$), $\alpha_\perp$ changes its sign twice. We call attention to the fact that the $\alpha_\perp(T)$ anomalies fall in that c/a region where the ETT appear at the K point. The general thermodynamic expressions for the thermal expansion of uniaxial crystals can be written as

$$\alpha_\perp=(c_{33}X_\perp-c_{13}X_\parallel)/c^*,$$

$$\alpha_\parallel=[(c_{11}+c_{12})X_\parallel-2c_{13}X_\perp]/c^*,$$

where c_{ij} are the isothermal elastic constants, $c^*=c_{33}(c_{11}+c_{12})-2(c_{13})^2$, $X_\perp=\frac{1}{2}(1/V)(\partial S/\partial \ln a)_{T,c}$, $X_\parallel=(1/V)(\partial S/\partial \ln c)_{T,a}$, and S is the entropy. The entropy from electrons S_{el} and phonons S_{ph} is closely associated with the density of states of electrons $N(E_F)$ and with the spectral density of states of phonons $\mathcal{G}(\omega)$,

$$S_{el}=\frac{\pi^2}{3}k_B^2TN(E_F),$$

$$S_{ph}=k_B\int_0^\infty[x\coth x-\ln(2\sinh x)]\mathcal{G}(\omega)d\omega,$$

where ω is the frequency of phonons, $x=\hbar\omega/2kT$, and k_B is the Boltzmann constant. Both the ETT and the Kohn anomaly destruction (as a result of the ETT) can lead to singularities in the density of states of electrons and phonons (the van Hove singularities) which affect $X_\perp$ and $X_\parallel$. The elastic constant dependences on the temperature for Zn are regular and show no unusual behavior.[25] Hence, the anomalies of $\alpha_\perp(T)$ are related solely to the behavior of $X_\perp(T)$ and $X_\parallel(T)$. For Zn, c_{13} is less than c_{33} but very close to it, and $X_\parallel>X_\perp$ for anisotropic crystals. As a consequence, $c_{33}X_\perp\approx c_{13}X_\parallel$, and the observed oscillation of $\alpha_\perp(T)$ at low temperatures results from a delicate balance between $c_{33}X_\perp$ and $c_{13}X_\parallel$.

In summary, our calculations show that the band level E_K at $c/a\simeq1.82$ intersects E_F and the needles occur around the point K of the Brillouin zone. This ETT correlates with the crossing effects for the electrical and thermal resistivities as well as with the sign change of the thermal-expansion coefficient $\alpha_\perp$. It is expected that the same effects should be observed when any passing the line $c/a\approx1.82$ on the T-P diagram (Fig. 4).

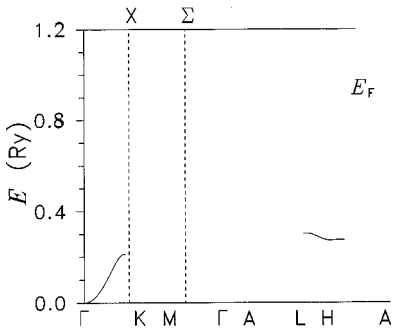

FIG. 5. Electron energy bands along the symmetry direction of the Brillouin-zone boundary surface for hcp Zn at the relative volume ratio $V/V_0=0.8932$ ($c/a=\sqrt{3}$). The dashed lines correspond to the X and Σ symmetry points of the Jones zone.

B. ETT at the L point of the Brillouin zone

Our calculations show that the doubly degenerated upper edge E_L intersects the Fermi level at $c/a\approx1.732$ (Fig. 1). Due to the spin-orbit splitting, two ETT, namely, two pieces of the Fermi surface, the ''butterfly'' and the ''cigar'' (from the third and the fourth zones, respectively) appear simultaneously around the L symmetry point of the Brillouin zone. The appearance of these ETT's corresponds to the minimum of the total density of states at the Fermi level, $N(E_F)$ (Fig. 3). Figure 5 illustrates the band structure of hcp Zn for this specific c/a ratio.

Lynch and Drickamer have studied the electrical resistance R of Zn under high pressure at 300 K.[17,30] Their data up to 16 GPa as well as the results of our computations of $N(E_F)$ are shown in Fig. 3. The excellent correlation between $N(E_F)$ and R as a function of pressure is quite remarkable: the minimum and abnormal increases of R under pressure correspond to those of $N(E_F)$. The resistivity $\rho=m^*/ne^2\tau$ may be expressed in the explicit form of $N(E_F)$ since the reverse time relaxation may be written as

$$\frac{1}{\tau}=\frac{\pi VN(E_F)}{\hbar k_F^4}\int_0^{2k_F}dq|S(q)v(q)|^2q^3,$$

where $v(q)$ is the pseudopotential form factor and $S(q)$ is the structure factor. The above expression shows that the resistivity is directly proportional to the density of states (see also Ref. 31). It may be inferred that the unusual resistance behavior under pressure is a consequence of the ETT at the L point.

It should be emphasized that at $c/a<1.732$ the Fermi surface of Zn contains all of the six elements, as for Mg with the axial ratio close to the ideal one (Fig. 4). The hcp structure at the axial ratio $\sqrt{3}$ has a peculiar symmetry both in the real and reciprocal spaces. In the reciprocal space, at $c/a=\sqrt{3}$ the $\Gamma\Gamma$ and ΓM distances in the first Brillouin zone become equal, causing the coincidence of [002] and [100] reciprocal-lattice vectors. In the real space, the hcp structure can be also

represented by the orthorhombic one with four atoms in the unit cell. At the axial ratio $c/a=\sqrt{3}$, the orthorhombic cell transforms to the tetragonal one, and two groups of symmetry, hexagonal and tetragonal, coexist simultaneously.

The axial ratio singularity at the $c/a=\sqrt{3}$ detected by Takemura from the x-ray diffraction experiments[6,8] was reproduced at the $c/a\approx\sqrt{3}$ region in the total-energy calculations for equilibrium lattice parameters.[12–15] Explanations of the reason for this anomaly are controversial. Thus, Fast *et al.*[12] concluded that the appearance of needles around the *K* points at $c/a\approx\sqrt{3}$ is responsible for the anomaly. At the same time, Novikov *et al.*[13] argued that not the ETT, but a local enhancement of $N(E_F)$, was a source of anomalies in Zn. They claimed, unlike the calculations of Godwal *et al.*,[14] that the band level at the point *L* never falls below E_F in Zn (and Cd) even for the highest pressure. Later, in contrast to their previous conclusions, Novikov *et al.*[15] asserted that *three* ETT's occurred simultaneously at $V/V_0\approx0.88$. Two of them were connected with the saddle point and with the needles at the *K* point and the third one with the butterfly at the *L* point.

Very recently Takemura[32] have reported the results of high-pressure x-ray diffraction experiments of Zn at room temperature with helium pressure medium.[33] The experiments have demonstrated regular behavior in the c/a axial ratio under pressure without any anomalies. What is most remarkable is that the anomaly of the c/a with methanol-ethanol-water (MEW) pressure medium[6,8] occurs at $c/a\approx\sqrt{3}$, i.e., in the region, where the electronic spectrum, lattice dynamics, and crystalline structure of Zn is distinctive. The total-energy calculations by Novikov *et al.*[13] show that the total energy in the ''anomaly region'' is essentially flat at finite temperature and show a double-well structure at low temperature [i.e., that at $T=0$ the structural change at $c/a\approx1.73$ is a first-order (isostructural) transition]. It is conceivable that c/a anomaly[6,8] at 300 K and the drastic drop of the Lamb-Mössbauer factor[4,5] at 4.2 K observed in Zn with MEW pressure medium are closely related to the specific dependence of the total energy of Zn in the anomaly region.

III. CONCLUSIONS

Our calculations of the electronic structure and density of states for hcp Zn show that three ETT's occur in Zn when c/a reduces. One of the transitions occurs at $c/a\approx1.82$ when the needles appear around the symmetry point *K* of the Brillouin zone. The other two transitions occur at $c/a\approx1.73$, when the butterfly and cigar appear simultaneously both around the *L* point. One can recognize three electronic phases on the *T*-*P* diagram of Zn at $P<10$ GPa. The lines $c/a\approx1.82$ and $c/a\approx1.73$ on this diagram are the boundaries between electronic phases. It is particularly remarkable that the electronic phase at $c/a<1.73$ contains a complete set of the Fermi-surface elements, as for the nearly-free-electron model. The ETT's correlate with a number of anomalies observed in Zn under compression.

The intersection of electrical resistivities ($\rho_\parallel$ and $\rho_\perp$) at $P\simeq1.29$ GPa ($T=300$ K) and the thermal resistivities ($w_\parallel$ and $w_\perp$) at thermal compression ($T\simeq30$) K, as well as the sign change of the linear thermal expansion coefficient $\alpha_\perp$ at low temperature and ambient pressure occurred at the c/a axial ratio when the ETT appear at the point *K*.

The double ETT's around the *L* point at $c/a\approx1.73$ correspond to the minimum of the density of states, $N(E_F)$, and correlate excellently with the minimum and abnormal increases of the electrical resistance under pressure. We predict that a number of transport and thermodynamic properties change (as, for example, in the case of the ETT at the *K* point) when passing the line $c/a\approx1.73$ on the *T*-*P* diagram.

ACKNOWLEDGMENTS

I am grateful to Dr. Takemura Kenichi for communicating his experimental x-ray data prior to their publication and for a very useful discussion. I am also grateful to Professor I. S. Itskevich, Dr. N. I. Kulikov, Dr. S. V. Popova, and Dr. A. P. Kochkin for fruitful discussions. This work was supported by the Russian Foundation for Basic Research, Project No. 00-02-16019.

*Electronic address: kechin@ns.hppi.troitsk.ru

[1] S. Daniuk, T. Jarlborg, G. Kontrym-Sznajd, J. Majsnerowski, and H. Stachowiak, J. Phys.: Condens. Matter **1**, 8397 (1989).

[2] I.M. Lifshits, Zh. Éksp. Teor. Fiz. **38**, 1569 (1960) [Sov. Phys. JETP **11**, 1130 (1960)]; A.A. Varlamov and A.V. Pantsulaya, *ibid.* **89** 2188 (1985) [*ibid.* **62**, 1263 (1985)]; V. Antropov, M.I. Katsnelson, V.G. Koreshkov, A.I. Likhtenstein, A.V. Trefilov, and V.G. Vaks, Phys. Lett. A **59**, 693 (1994); M.I. Katsnelson, I.I. Naumov, and A.V. Trefilov, Phase Transit. **B49**, 143 (1994).

[3] The ETT was originally identified under pressure just in hcp Cd [E.S. Itskevich and A.N. Voronovskii, Zh. Éksp. Teor. Fiz. Pis'ma Red. **4**, 226 (1966) [JETP Lett. **4**, 154 (1966)]; S.L. Bud'ko, A.N. Voronovskii, A.G. Gapotchenko, and E.S. Itskevich, Zh. Éksp. Teor. Fiz. **86**, 778 (1984) [Sov. Phys. JETP **59**, 454 (1984)]].

[4] W. Potzel, M. Steiner, H. Karzel, W. Schiessl, M. Köfferlein, G.M. Kalvius, and P. Blaha, Phys. Rev. Lett. **74**, 1139 (1995).

[5] M. Steiner, W. Potzel, H. Karzel, W. Schiessl, M. Köfferlein, G.M. Kalvius, and P. Blaha, J. Phys.: Condens. Matter **8**, 3581 (1996).

[6] K. Takemura, Phys. Rev. Lett. **75**, 1897 (1995).

[7] K. Takemura (private communication).

[8] K. Takemura, Phys. Rev. B **56**, 5170 (1997).

[9] O. Schulte and W.B. Holzapfel, Phys. Rev. B **53**, 569 (1996).

[10] J.G. Morgan, R.B. Von Dreele, P. Wochner, and S.M. Shapiro, Phys. Rev. B **54**, 812 (1996).

[11] S. Klotz, M. Braden, and J.M. Besson, Phys. Rev. Lett. **81**, 1239 (1998).

[12] L. Fast, R. Ahuja, L. Nordstrom, J.M. Wills, B. Johansson, and O. Eriksson, Phys. Rev. Lett. **79**, 2301 (1997).

[13] D.L. Novikov, A.J. Freeman, N.E. Christensen, A. Svane, and C.O. Rodriguez, Phys. Rev. B **56**, 7206 (1997).

[14] B.K. Godwal, E. Meenakshi, and R.S. Rao, Phys. Rev. B **56**, 14 871 (1997).

[15] D.L. Novikov, M.I. Katselson, A.V. Trefilov, A.J. Freeman, N.E.

Christensen, A. Svane, and C.O. Rodriguez, Phys. Rev. B **59**, 4557 (1999).
[16] A.V. Overhauser, Phys. Rev. Lett. **81**, 4022 (1998).
[17] R.W. Lynch and H.G. Drickamer, J. Phys. Chem. Solids **26**, 63 (1965).
[18] A.N. Ivanov, V.V. Kechin, A.I. Likhter, and E.M. Ogneva, High Temp.-High Press. **7**, 656 (1975).
[19] E. Goens and H.M. Grüneisen, Ann. Phys. (Leipzig) **14**, 164 (1932); K. Mendelssohn and H.M. Rosenberg, Proc. Phys. Soc., London, Sect. A **65**, 385 (1952).
[20] R.D. McCammon and G.K. White, Philos. Mag. **11**, 1125 (1965).
[21] O.K. Andersen, Z. Pawlowska, and O. Jepsen, Phys. Rev. B **34**, 5253 (1986).
[22] H.J. Nowak, O.K. Andersen, T. Fujiwara, O. Jepsen, and X. Vargas, Phys. Rev. B **44**, 3577 (1991).
[23] O.K. Andersen, O. Jepsen, and M. Sob, *Electronic Band Structure and its Applications*, edited by Lecture Notes in Physics Vol. 283 (Springer, Berlin, 1997); O.K. Andersen, *Methods of Electronic Structure Calculations* (Singapore, World Scientific, 1994).
[24] E. Bodenstedt, B. Perscheid, and S. Nagel, Z. Phys. B: Condens. Matter **63**, 9 (1963).
[25] C.W. Garland and R. Dalven, Phys. Rev. **111**, 1232 (1958).
[26] V.A. Rowe and P.A. Schroeder, J. Phys. Chem. Solids **31**, 1 (1970).
[27] W.J. O'Sullivan and J.E. Shirber, Phys. Rev. **151**, 484 (1966).
[28] V.A. Venttsel', O.A. Voronov, A.I. Likhter, and A.B. Rudnev, Zh. Éksp. Teor. Fiz. **52**, 617 (1967) [Sov. Phys. JETP **38**, 1220 (1974)].
[29] A.S. Ivanov, N.I. Mitrofanov, V.V. Pushkarev, A.Y. Rumyantsev, and N.A. Chernoplekov, Fiz. Tverd. Tela (Leningrad) **28**, 767 (1986) [Sov. Phys. Solid State **28**, 427 (1986)].
[30] Here we use a new pressure scale [H.G. Drickamer, Rev. Sci. Instrum. **41**, 1667 (1970)].
[31] N.I. Kulikov, J. Phys. F: Met. Phys. **8**, L137 (1978).
[32] K. Takemura (unpublished), p. 150.
[33] It should be noted that the pressures at $T \leqslant 300$ K and $P > 12$ GPa are quasihydrostatic, since at these conditions all pressure mediums, even helium, are solid [F. Datchi, P. Loubeyre, and R. LeToullec, (unpublished).